J Mol Model (2011) 17:2873–2882
DOI 10.1007/s00894-011-0982-y

ORIGINAL PAPER

A computerized protein–protein interaction modeling study of ampicillin antibody specificity in relation to biosensor development

Minghua Wang · Jianping Wang

Received: 10 October 2010 / Accepted: 21 January 2011 / Published online: 11 February 2011

Abstract Nonspecific interactions between immobilized biomolecules and interfering proteins significantly impede biosensor development and commercialization. Advances in bioinformatics and computer technology have facilitated a greater understanding of biological interactions. We employed two different protein–protein docking programs to simulate the nonspecific interaction between ampicillin antibody and potential interfering proteins (human serum albumin and ovalbumin). To evaluate the contact and probability of association with the active site of the antibody, different amino acid chains from human serum albumin (HSA) and ovalbumin (OVA) were modeled in the simulation. In addition, a well-known specific immune complex, lysozyme and lysozyme antibody, was simulated for comparison. The results demonstrated that the cluster density of nonspecific interactions was smaller than the specific interaction between lysozyme and antibody, and that the dock scores were scattered. However, the active site of ampicillin antibody was prone to nonspecific protein interactions. The strength of interaction was different for specific binding and nonspecific binding. These results provide a platform for detecting the probability of nonspecific interactions and for improving methods of biosensor detection construction with reduced nonspecific adsorption.

Keywords Computer · Ampicillin antibody · Bovine serum albumin · Nonspecific interaction · Protein–protein docking

M. Wang · J. Wang (✉)
College of Biosystems Engineering and Food Science,
Zhejiang University,
Hangzhou 310029, China
e-mail: jpwang@zju.edu.cn

Introduction

Advances in biotechnology have yielded a plethora of commercial products that rely on biomolecular interactions. Biosensors are useful analytical tools for basic research, and they have many practical and commercial applications in medicine, environmental protection, and food safety [1–5]. Two crucial factors in the applicability of a biosensor are the sensitivity and the specificity of the immobilized biological molecules that detect analytes. Specificity is conferred by two types of interactions: those at the interface of the biotic and supporting abiotic components, and those between the biomolecule-recognizing element and the analyte [6, 7]. An immunosensor is a common type of biosensor that exploits the specific molecular recognition of an antigen by an antibody [8]. For some small chemical analytes with low antigenicity, it is often necessary to use chemical–protein conjugates for antibody production. In addition, to improve and stabilize the biosensor, many applications use bovine serum albumin (BSA) or ovalbumin (OVA) as a binding protein for antigen immobilization [9–12]. BSA also serves as a blocking solution to occupy excess binding sites on the electrode [13–16]. Serum albumin is a common and abundant protein in the animal hematologic system that transports drugs, nutriments, and other blood-borne molecules. Thus, in order to detect antibiotic residues in food or the environment using a biosensor, it is necessary to evaluate the adsorption of BSA on the supporting surface, and the affinities of BSA and OVA for the antibody.

Due to technological innovations in bioinformatics, a wealth of experimental and theoretical structural data has become available, and the number of therapeutically relevant macromolecular structures is growing rapidly [17]. Molecular simulation is a complementary approach to research in chemistry and biochemistry that is based on the use of

quantum mechanics (QM), molecular mechanics (MM), and the high computational capacities of advanced computer systems [18, 19]. Compared with experimental methods, computational studies have some advantages, such as lower research costs, greater safety, the ability to study molecular interactions on very fast time scales, and high reproducibility. Jeyachandran et al. [20] studied the adsorption/desorption of BSA on hydrophilic and hydrophobic surfaces. They modeled the adsorption in silico using the Material Studio software package, and simulations were found to give results in accord with experimental results. Molecular simulation has also been used to study protein–protein binding, such as enzyme–substrate and antibody–antigen interactions. In addition, other special software packages have been developed [21]. Although there are experimental and computational challenges in this field [22], these new research methods could facilitate biosensor development by permitting detailed investigations of biomolecule recognition at the interfaces of supported materials, as well as the interference caused by other proteins.

In simulations of protein–protein interactions, the basic input data are derived from protein crystallography and sequence analysis. Interactions are modeled based on shape complementarity, electrostatics interactions, and other relevant biochemical information. The ZDOCK algorithm models initial-stage docking and optimizes desolvation, pairwise shape complementarity (PSC), and electrostatics using a fast Fourier transform (FFT) method, and it has been shown to accurately predict many functional protein interactions [23, 24]. Most studies have focused on specific functional protein interaction simulations. However, many nonspecific protein interactions can interfere with biosensor responses, so they require further experimental and theoretical study. In this report, we employed ZDOCK to predict nonspecific interactions between ampicillin antibody and human serum albumin (HSA)/ovalbumin (OVA) in order to improve ampicillin residue detection by immunosensors and to evaluate a computer-aided methodology for simulating and analyzing nonspecific interactions between proteins.

Computational protein–protein docking methods

The 3D structures of ovalbumin, the lysozyme antibody complex, and the ampicillin antibody complex were downloaded from the Protein Data Bank (the PDB codes were 1OVA, 1JTT, and 1H8S). The crystal structure of BSA was not included in the PDB, so we used the 3D structure of HSA (PDB code, 1AO6), as it has 76% amino acid sequence identity with BSA [25].

We choose two different in silico methods to study the docked complex. FiberDock [26] (http://bioinfo3d.cs.tau.ac.il/FiberDock) is a solution for docking that models backbone flexibility via an unlimited number of normal modes. We uploaded PDB file 1H8S (ampicillin antibody) as the receptor and PDB files 1AO6 (HSA) and 1OVA (OVA) as ligands for docking simulations without any binding chains and parameter alterations. The custom parameters, including "backbone refinement," "backbone flexibility level," "rigid-body optimization (number of MC cycles)," and "atomic radius scale" were set to their default values.

We defined ampicillin antibody chain A as the receptor for binding as well as chain A of HSA and chain A of OVA as the ligands for binding using the ZDOCK program package integrated into Discovery Studio 2.1. In addition, another docking simulation between chain B of the ampicillin antibody (receptor) and chain A of HSA (ligand) was performed by ZDOCK. Before the ZDOCK runs, the PDB files were treated with "protein reports and utilities tools" to split the protein structure and to add hydrogen atoms and termini to the proteins. The ZDOCK program [23, 27] is an initial-stage docking algorithm that provides near-native structure predictions. It employs three steps: a search procedure, blocking and filtering, and the processing of possible poses by clustering. The search procedure exhaustively searches all rotational and translational spaces for the ligand protein relative to the receptor protein, which is fixed at its starting orientation. Filtering is used to eliminate conformations that do not include the specified residue(s) at the interface by defining atoms that are within or beyond a cut-off distance. The clustering of the docked poses is based on an all-against-all RMSD matrix. The RMSD between two docked poses is calculated based on the ligand residues within a user-specified distance of the binding interface. Therefore, we chose the following ZDOCK parameters: the "distance cut-off" when filtering poses was 10.0 Å, the top 2000 poses were used for clustering, the "RMSD cut-off" and the "interface cut-off" for clustering were both 10.0 Å, and the "maximum number of clusters" was 60. Other parameters were kept at their default values. We then conducted computational trials to compare the different protein–protein docking results.

In order to evaluate the validity of the docking method for simulating nonspecific protein–protein interactions, we first performed specific antibody–antigen docking by ZDOCK for a well-known immune complex, lysozyme and lysozyme antibody (PDB code 1JTT).

Results and analysis

Protein–protein interaction simulation by FiberDock

The 3D structures of many protein complexes are now available and can be used to model other enzyme–substrate and antibody–antigen interactions. A greater understanding of these biological processes will benefit clinical medicine and biological product applications.

As it is a small molecule, the preparation of an ampicillin antibody necessitates the conjugation of ampicillin to BSA or OVA in order to confer immunogenicity [28–30]. FiberDock is an efficient method for flexibly refining and re-scoring rigid-body protein–protein docking solutions. The method iteratively minimizes the structure of the flexible protein along the most relevant modes. The relevance of a mode is calculated based on the correlation between the chemical forces applied to each atom and the translational vector of each atom, according to the normal mode. Figure 1 displays the reported best simulation result for the antibody–HSA interaction. The full protein–protein complex is depicted on the left; this shows that only the two A chains participate in the interaction while the B chains remain in their natural configurations. The right panel in Fig. 1 shows the HSA and antibody residues that are closest together. The figure also shows the aspartic acid and asparagine (Asp, Asn), glutamic acid and glutarnine (Glu, Gln), arginine (Arg), tryptophan (Trp), and tyrosine (Tyr) residues that appear in the active region.

OVA is another binding protein that is often conjugated to small drugs such as antibiotics and toxins for enhanced antigenicity. It has four amino acid chains, two of which interact with all antibody proteins. Figure 2 illustrates the protein–protein docking result for ampicillin antibody and OVA. We can see that two A chains of the two proteins interact in the docked complex. The antibody's active site lies in chain A.

Protein–protein interaction simulation using ZDOCK

The results of the FiberDock simulations indicated that for full antigen coupling between protein and antibody, the complementarity-determining regions (CDRs) of the antibody tended to bind to HSA and OVA. The next questions to address were whether this interaction was nonspecific and whether antibody chain B could also bind to HSA. The 3D structure of 1H8S [30] comes from ampicillin antibody prepared using an ampicillin–BSA conjugate (used to immunize mice), so we also wanted to see whether this influenced the affinity of the antibody for OVA. We used ZDOCK to study the binding affinities of different antibody amino acids in the other protein chains present during nonspecific interactions.

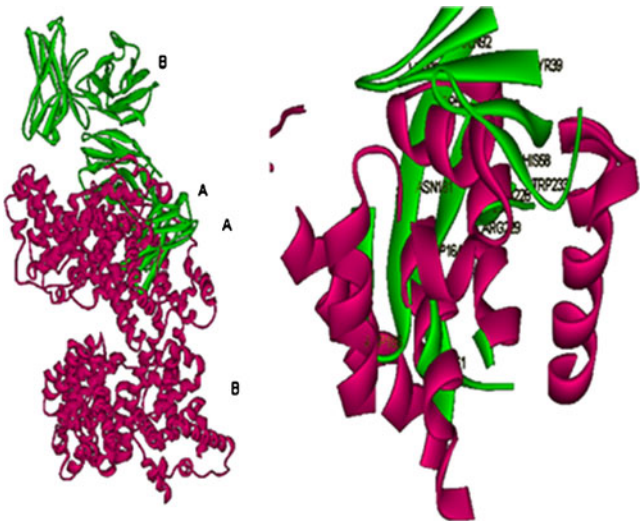

Fig. 1 Simulation result for the ampicillin antibody–HSA interaction. *Left*, full protein–protein complex; *right*, HSA and antibody residues that are closest together. *Green* antibody, *purple* HSA

Fig. 2 Simulation result for the ampicillin antibody–OVA interaction. *Green* antibody, *purple* OVA)

The ZDOCK results provided 2000 docked poses that rely on atomic motions simulated by the molecular force field. Evaluating the properties of an ensemble of docked structures through clustering can help to filter these docked poses [31, 32]. Each possible pose was analyzed statistically by clustering based on an all-against-all RMSD matrix. Figure 3 shows the cluster density for each docked protein complex. Around 1200 docked poses with nonspecific interactions and 1600 lysozyme–antibody poses were included among the 60 clusters. The poses with the specific interaction between antibody and lysozyme mostly occurred in the top 20 clusters, with about 400 located in the first three clusters and a total of 1040 poses present in the top 20 clusters. In contrast, poses with nonspecific interactions were decentralized, especially chain B of the ampicillin antibody when interacting with HSA. The number of these poses in the top 20 clusters was small (580 for chain A and 560 for chain B; see Fig. 3a and b). For the interaction of ampicillin antibody with OVA, we focused on chain A of the ampicillin antibody. The interaction between the two A chains is shown in Fig. 3d. The cluster density was similar to those found for the interactions represented by Fig. 3a and b. In particular, the

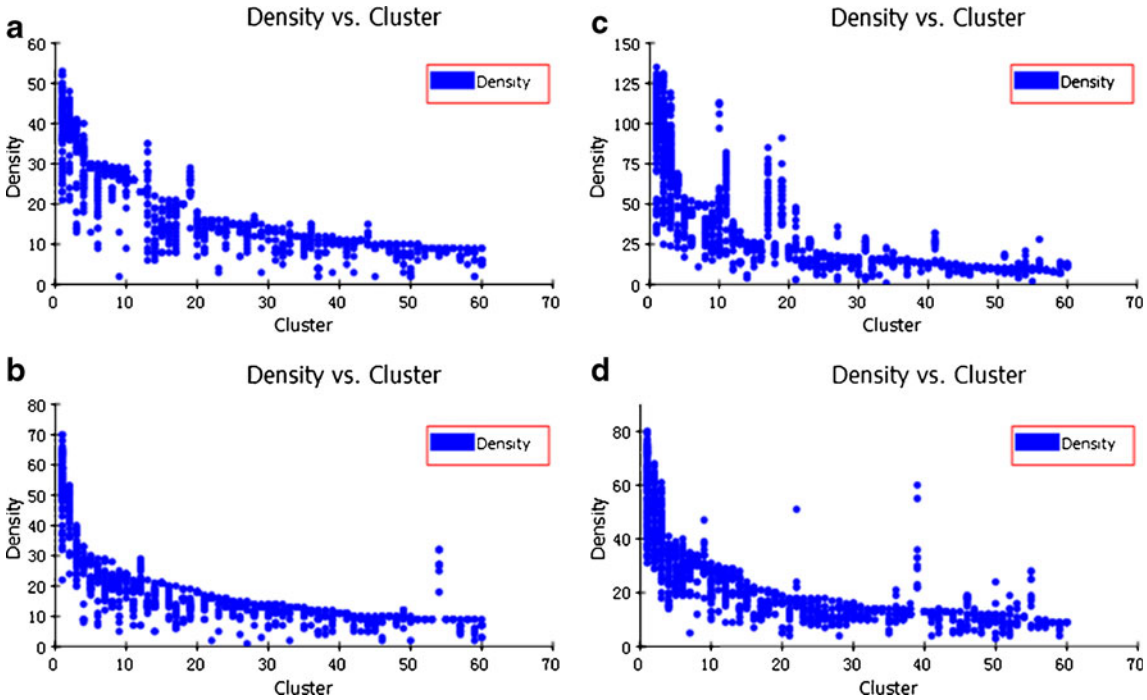

Fig. 3a–d ZDOCK cluster densities in different protein–protein interaction simulations: **a** ampicillin antibody chain A and HSA chain A, **b** ampicillin antibody chain B and HSA chain A, **c** lysozyme and antibody, PDB code 1JTT, **d** ampicillin antibody chain A and OVA chain A

first three clusters were similar. There were about 700 poses in the top 20 clusters. This indicated that there was a greater probability of the specific interaction occurring than nonspecific interactions. In another words, protein–protein interaction simulations in computer-aided studies can shed light on biosensor performance during both specific and nonspecific interactions, and can be used to assess the probability of both.

Although the simulation of ampicillin antibody chain A and OVA chain A gave a larger number of poses among the top 20 clusters, the ZDock score was reversed. The ZDock score is the shape complementarity score calculated by the ZDOCK program, and includes electrostatics and desolvation energy terms. Higher scores are better. The dock scores of the ampicillin antibody chain A and OVA chain A poses (Fig. 4d) were the lowest among these four complexes, followed by 1H8S chain B and HSA chain A poses (Fig. 4b), while the poses of ampicillin antibody chain A binding to HSA gave the highest ZDock scores (Fig. 4a). This result corresponded to the FiberDock result for full protein recognition, so the method used to prepare the antibody (i.e., the conjugate used) may affect specificity. However, for the specific interaction of the biomolecule, although lysozyme and its antibody gained a more intensive score (13~18) than ampicillin antibody chain A binding to HSA (16~26), its score were lower. This result demonstrated that the antibody's active site can be influenced by the nonspecific interaction probability.

Biomolecular association is thought to occur in two steps: encountering and then docking through the formation of specific contacts and noncovalent bonds. Electrostatic interactions would therefore be expected to directly influence both the initial association (through steering) and the strength of the docked complex (through salt bridges and hydrogen bonds). For special immune reactions, electrostatic interactions are also significant. Electrostatic differences at antibody–antigen binding sites should have important implications for specificity and cross-reactivity. Researchers have reported that there are large differences among the three specific antibody and lysozyme complexes in their electrostatic binding components [33].

ZRANK [34] is a method for quickly and accurately re-ranking the docked protein complexes predicted by the ZDOCK rigid body docking program. ZDOCK predictions are made based on desolvation free energy and electrostatic force. The aqueous solvent is an important part of any protein–protein system. At binding sites, individual water molecules can influence the binding affinity, while in the bulk solvent, the polarization, reorganization, and orientations of water molecules can make it difficult to characterize bulk–solvent electrostatic effects quantitatively. The process of desolvation involves these important bulk solvation effects. ZDOCK estimates desolvation based on the atom contact energy (ACE). The ACE is defined as the free energy necessary to replace two protein atom–water contacts with the corresponding protein atom–protein atom and water–water contacts. Figure 5 shows the solvation effect simulations. We found that the specific interaction

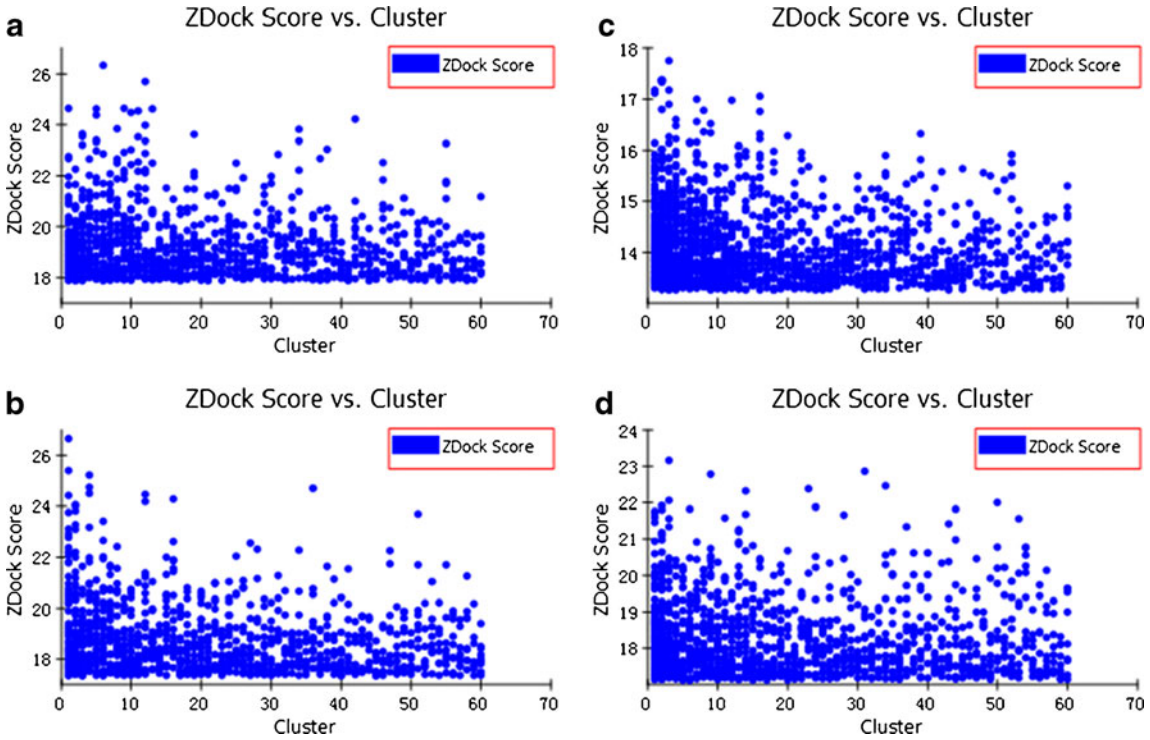

Fig. 4a–d ZDock scores from different protein–protein interaction simulations: **a** ampicillin antibody chain A and HSA chain A, **b** ampicillin antibody chain B and HSA chain A, **c** lysozyme and antibody, PDB code 1JTT, **d** ampicillin antibody chain A and OVA chain A

between lysozyme and lysozyme antibody (Fig. 5c) has a relatively low and intensive solvation free energy (−10 to 20 kcal mol^{-1}). For the other three interactions, the solvation effects associated with Fig. 5a and b (about 0–60 kcal mol^{-1}) are larger than those associated with Fig. 5d (−10 to 40 kcal mol^{-1}), which in turn are nearest to those associated with Fig. 5d (i.e., a≈b > d>c).

Figure 6 illustrates the electrostatic interactions of the various associated biomolecules. Figure 6a shows greater electrostatic interactions than Fig. 6c and d (similar to ranking seen for the solvation free energies in Fig. 5). This demonstrates the relationship between solvation and electrostatic interactions. Van der Waals (VdW) contact refers to the treatment of the core–core repulsion and the attractive van der Waals dispersion interactions between different atoms. The VdW contact was calculated between all atom pairs within a user-specified interatomic cut-off distance (10.0 Å in this work), except for covalently bonded atom pairs and atom pairs separated by two covalent bonds. Van der Waals force effects were usually considered with electrostatic interactions, and they showed a cooperative effect.

Figure 7 illustrates the VdW contacts of different complexes. The specific interaction between lysozyme and antibody had the highest value (−100 to 0 kcal mol^{-1}), while the other three reactions gave lower or similar values. The complex poses associated with Fig. 7a and d, which both include the antibody's active site, have higher values than the poses associated with Fig. 7b. Thus, these results are similar to those shown in Fig. 5 too. These factors mainly act on the atoms of unbound proteins. In order to evaluate the interactions with active sites, water molecules and amino acid atoms should be taken into account.

ZDock scores based on grid-based shape complementarity and desolvation showed that a nonspecific interaction between HSA and ampicillin antibody was highly probable due to shape complementarity. The effects of desolvation and electrostatic forces on the ZDock scores are less obvious, and the cluster density may be related to these factors. Thus, the docking simulation indicated that nonspecific interactions should occur between the ampicillin antibody and interfering ground proteins, and the antibody's active site is a favorable binding site. In addition, these results provide a theoretical basis for evaluating and controlling the probability of nonspecific adsorption during biosensor analytical processes.

Discussion

The high specificities and efficiencies of immunoreactions have been exploited in biomolecule sensing and analysis; for example, food safety determination involves the detection of trace amounts of undesired compounds like

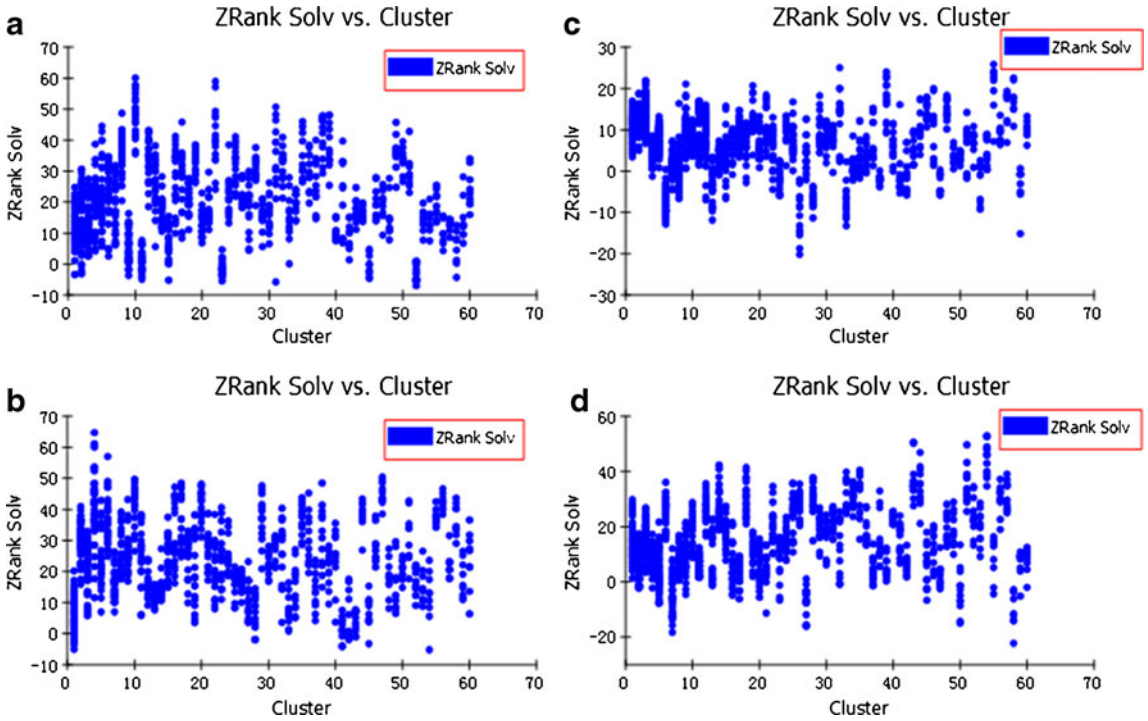

Fig. 5a–d ZRank desolvations of different protein–protein interaction simulations: **a** ampicillin antibody chain A and HSA chain A, **b** ampicillin antibody chain B and HSA chain A, **c** lysozyme and antibody, PDB code 1JTT, **d** ampicillin antibody chain A and OVA chain A

residual veterinary antibiotics. These contaminants are often small molecules, so BSA or OVA must be used for antibody production. We focused on the development of an ampicillin residue detection immunosensor, and Fig. 8a shows a schematic of the preparation of this antibody. Thus, the prepared ampicillin antibody may also possess BSA and/or OVA affinity that could influence an antibody-based analytical method. Immunosensors often utilize two main

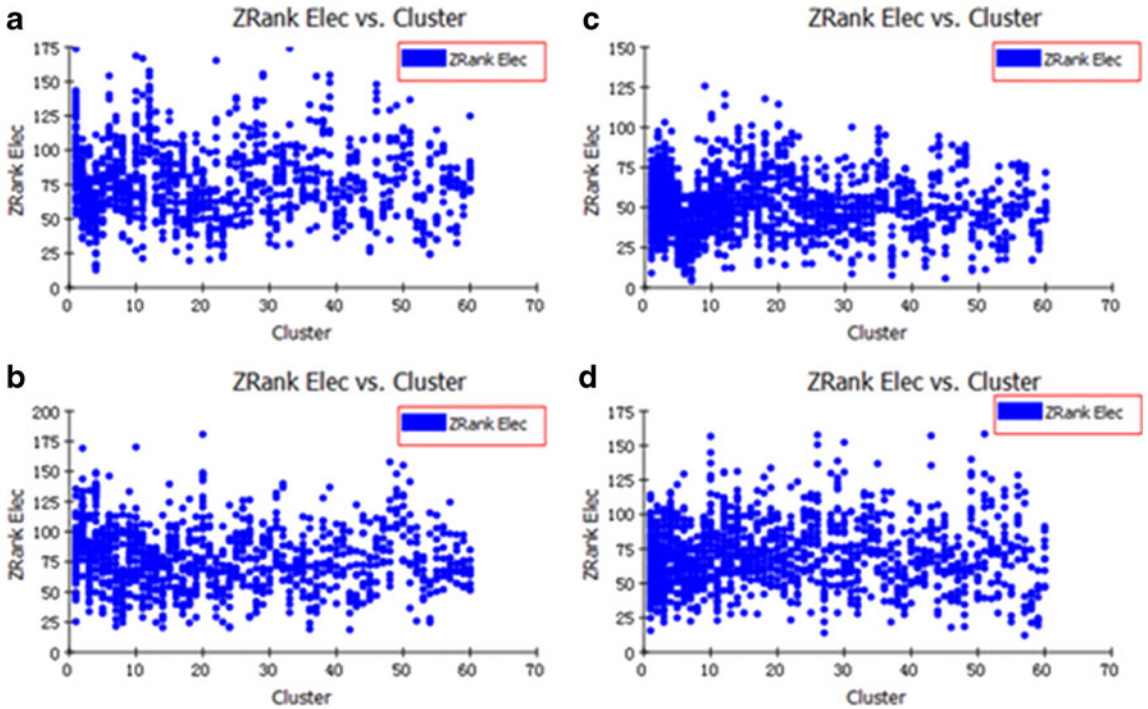

Fig. 6a–d ZRank electrostatic effects in the different protein–protein interaction simulations: **a** ampicillin antibody chain A and HSA chain A, **b** ampicillin antibody chain B and HSA chain A, **c** lysozyme and antibody, PDB code 1JTT, **d** ampicillin antibody chain A and OVA chain A

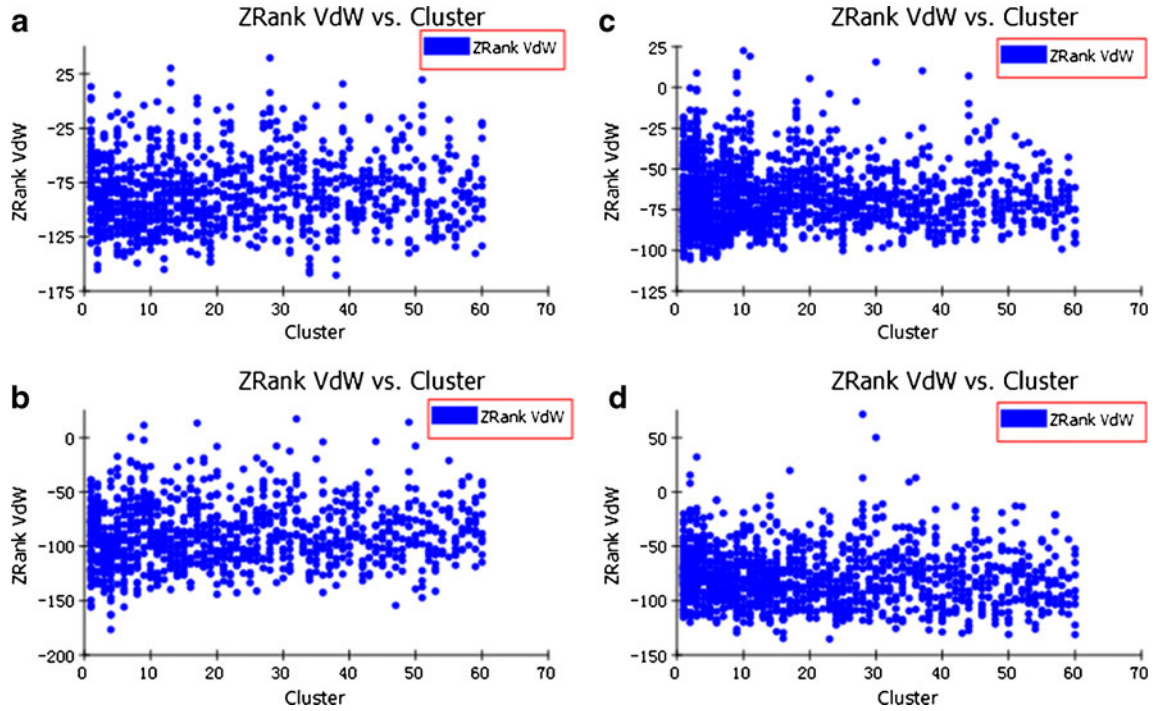

Fig. 7a–d Van der Waals contacts during different protein–protein interaction simulations: **a** ampicillin antibody chain A and HSA chain A, **b** ampicillin antibody chain B and HSA chain A, **c** lysozyme and antibody, PDB code 1JTT, **d** ampicillin antibody chain A and OVA chain A

formats: direct detection by the immobilized antibody and indirect detection by immobilized antigen coupling (as illustrated in Fig. 8b and c, respectively).

Figure 9 shows the chemical structure of the ampicillin antibody provided in the PDB. Figure 9a is the ampicillin–antibody complex. It has two protein chains; chain A provides a special cavity in its secondary or tertiary structure into which the ampicillin molecule embeds. Figure 9b shows the detailed binding features of ampicillin within the cavity based on the chemical and physical reactions between atoms of the antibody residues and ampicillin. The interactions include hydrogen bonds, hydrophobic interactions, electrostatic interactions, and van der Waals forces. Thus, the active site often includes aspartic acid and asparagine (Asp, Asn), glutamic acid and glutarnine (Glu, Gln), arginine (Arg), tryptophan (Trp), and tyrosine (Tyr) residues that tend to interact with side chains. Note that these residues are also found in Fig. 1. This implies that the active site of the ampicillin antibody can also participate in the interaction of the antibody with BSA.

Although there are some differences in the binding of a large protein and the binding of a small molecule, the docking results reveal some general rules. As shown in Fig. 8, BSA has been given before detection ampicillin residue, and if the antibody is bound to a large protein it should not bind to ampicillin. In the direct detection format, the efficiency and specificity of the immobilized ampicillin antibody was decreased by binding to the BSA used for blocking. In contrast, in the indirect format, despite immobilized antigen coupling or blocking by BSA, there are BSA and ampicillin molecules on the surface of the electrode. Therefore, the excess antibody in detection samples should bind to BSA or ampicillin, and the detection signal should not be influenced. Thus, for no BSA was contained in detection solution, although the efficiency was lower, the direct format seems accurately. The detection milk sample contained BSA would influence on both, and seriously to indirect one.

Bacigalupo et al. [35] developed an ampicillin haptenized-BSA immobilization-based time-resolved fluoroimmunoassay with a detection limit of 1 ng/ml. Samsonova et al. [36] reported an enzyme immunoassay based on polyclonal antibodies obtained by immunizing with ampicillin conjugated to BSA that could detect 5 ng/ml ampicillin in milk. Meyer [37] also reported a fully automated standalone flow-injection immunoanalysis (FIA) for the determination of cephalexin with a working range of 3–30 μg/L and an LOD of 1 μg/L, but BSA also appeared in the assay during the immune reaction. Chen et al. [38] reported a rapid enzyme-linked immunosorbent assay (ELISA) for cephalexin (CEX) residue detection based on a monoclonal antibody (mAb) against cephalexin–bovine serum albumin (CEX–BSA) conjugate as the immunogen. The detection limit of this rapid ELISA was calculated as 0.39 μg/kg. The ELISA used cephalexin–OVA (CEX–OVA) as the immobilized competitive antigen and 4% (w/v) skim milk in carbonate buffer as

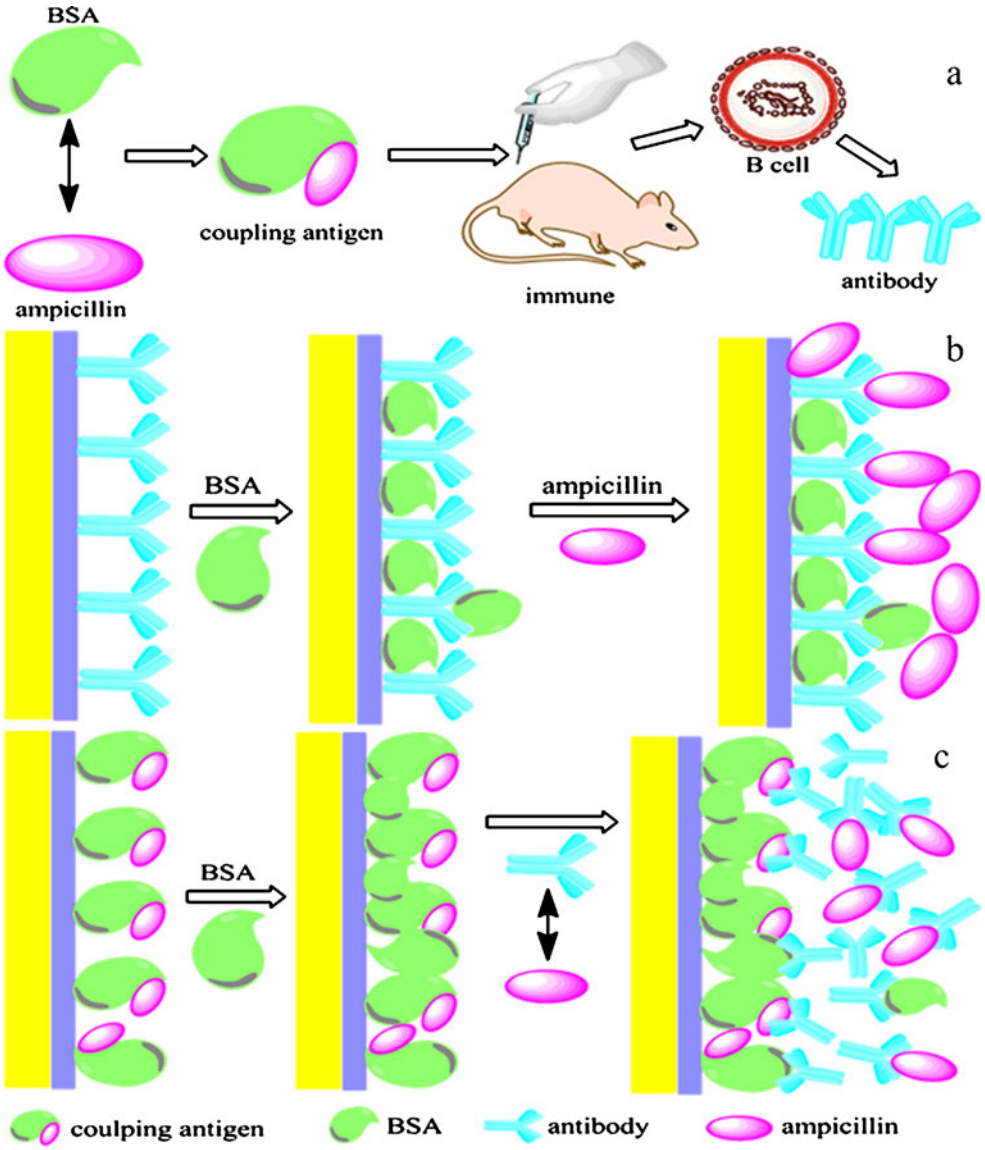

Fig. 8a–c Diagrams of immunosensor (**a** antibody production, **b** direct detection, **c** and indirect detection)

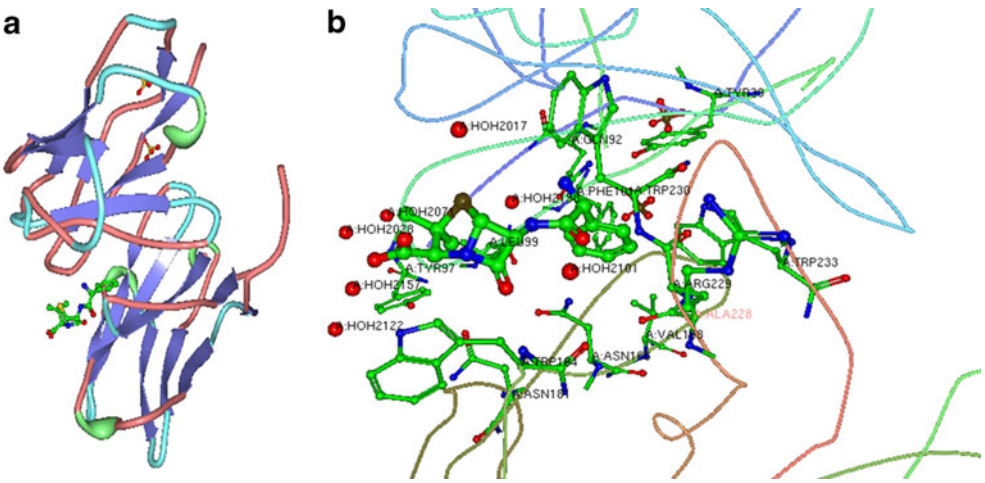

Fig. 9a–b Chemical structure of the ampicillin–antibody complex, as displayed in PDB (**a** shows the intact complex, **b** shows the closest residues of ampicillin and its antibody when complexed)

the blocking solution. Wu et al. [39] reported an amperometric immunosensor based on co-immobilizing new methylene blue (NMB) and horseradish peroxidase (HRP)-labeled penicillin pAb (Ab*) on a glassy-carbon electrode that had an LOD of 0.3 μg/L. However, they used gelatin as the blocking agent, and any BSA appearance should be founded during detection process. Thavarungkul et al. reported their work on a detector with a remarkably low LOD for penicillin G (3×10^{-15} M) [40]. Although it was based on monoclonal anti-penicillin G and label-free impedimetric flow-injection immune-reaction detection, it should be noted that they used 10 mM 1-dodecanethiol ethanol solution as the blocking agent rather than BSA. These research findings suggest potential interactions between antibodies and other non-detection target proteins that may influence biosensor performance. However, a detailed understanding of these effects is difficult to obtain.

The docking results provide evidence for potential interactions between antibodies and other non-detection target proteins. To improve immunosensor performance, BSA should not be used in both antibody production and antibody-modified electrode blocking. In the special case of contaminated milk detection, BSA and ampicillin co-occur. Once they are placed in competition on the binding surface, the interactions of the antibody, BSA, and ampicillin are complicated, presenting problems when attempting to model and interpret analytical test results.

Conclusions

This work focused on a computerized protein–protein interaction study, and aimed to obtain a detailed biomolecular recognition mechanism that is essential for the design and application of biosensors. Two different protein–protein interaction simulation methods were used to study nonspecific ampicillin antibody interactions. FiberDock results indicated that ampicillin antibody complementarity could lead to HSA or OVA binding and thus interfere with the biosensor preparation process and detection in samples containing these proteins. ZDOCK simulation was used for further evaluation of the docked protein–protein complexes. In comparison with the specific interaction between antibody and antigen (lysozyme and antibody), it was found that the cluster densities of nonspecific interactions between docking complexes were smaller but that the dock scores of these poses were more scattered. The nonspecific interaction between ampicillin antibody chain A and HSA presented a higher score than lysozyme and antibody, but chain B and HSA yielded a reasonably low score. In detection processes, specific biological reactions were occurred in kinds of protein solutions. Thus, solvation, electrostatic and van der Waals interactions are important in the formation of complexes. The probability of forming the antibody–OVA docking complex was lower than that for the antibody–HSA complex, implying that the antibody preparation method will affect the specificity. Computer-aided protein–protein interaction studies indicated that there was a potential nonspecific interaction between the immobilized biosensor antibody and HSA in the sample. The antibody's active site can participate in nonspecific protein interactions. The interaction strengths differed for specific and nonspecific binding. It is possible to develop and improve biosensors by employing a computerized simulation methodology. The antibody preparation method should also be considered carefully and its efficiency characterized. By highlighting the possibility of nonspecific binding, these modeling results may aid in the improvement of biosensor construction methods.

References

1. Matharu Z, Arya SK, Sumana G, Gupta V, Malhotra BD (2008) Self-assembled monolayer for low density lipoprotein detection. J Mol Recognit 21:419–424
2. Solanki PR, Prabhakar N, Pandey MK, Malhotra BD (2008) Nucleic acid sensor for insecticide detection. J Mol Recognit 21:217–223
3. Pol E, Karlsson R, Roos H, Jansson A, Xu BZ, Larsson A, Jarhede T (2007) Biosensor-based characterization of serum antibodies during development of an anti-IgE immunotherapeutic against allergy and asthma. J Mol Recognit 20:22–31
4. Meral Y, Hasan N, Gonul D (2010) A voltammetric *Rhodotorula mucilaginosa* modified microbial biosensor for Cu(II) determination. Bioelectrochemistry 79:66–70
5. Ryu SW, Kim CH, Han JW, Kim CJ, Jung C, Park HG, Choi YK (2010) Gold nanoparticle embedded silicon nanowire biosensor for applications of label-free DNA detection. Biosens Bioelectron 25:2182–2185
6. North SH, Lock EH, Taitt CR, Walton SG (2010) Critical aspects of biointerface design and their impact on biosensor development. Anal Bioanal Chem 397:925–933
7. Han PH, So PK, Ma DL, Zhao Y, Lai TS, Chung WH, Chan KC, Yiu KF, Chan HW, Siu FM, Tsang CW, Leung YC, Wong KY (2008) Fluorophore-labeled beta-lactamase as a biosensor for beta-lactam antibiotics: a study of the biosensing process. J Am Chem Soc 126:6351–6361
8. Jiang XS, Li DY, Xu X, Ying YB, Li YB, Ye ZZ, Wang JP (2008) Immunosensors for detection of pesticide residues. Biosens Bioelectron 23:1577–1587
9. Liu XP, Deng YJ, Jin XY, Jiang CLG, JH SGL, Yu RQ (2009) Ultrasensitive electrochemical immunosensor for ochratoxin A using gold colloid-mediated hapten immobilization. Anal Biochem 389:63–68
10. Long F, He M, Zhu AN, Shi HC (2009) Portable optical immunosensor for highly sensitive detection of microcystin-LR in water samples. Biosens Bioelectron 24:2346–2351
11. Kwon Y, Hara CA, Knize MG, Hwang MH, Venkateswaran KS, Wheeler EK, Bell PM, Renzi RF, Fruetel JA, Bailey CG (2008) Magnetic bead based immunoassay for autonomous detection of toxins. Anal Chem 80:8416–8423
12. Bone L, Vidal JC, Duato P, Castillo JR (2010) Ochratoxin A nanostructured electrochemical immunosensors based on poly-

clonal antibodies and gold nanoparticles coupled to the antigen. Anal Meth 2:335–341
13. Lian W, Wu DH, Lim DV, Jin SG (2010) Sensitive detection of multiplex toxins using antibody microarray. Anal Biochem 401:271–279
14. Sentandreu MA, Aubry L, Toldra F, Ouali A (2007) Blocking agents for ELISA quantification of compounds coming from bovine muscle crude extracts. Technol 224:623–628
15. Reimhult K, Petersson K, Krozer A (2008) QCM-D analysis of the performance of blocking agents on gold and polystyrene surfaces. Langmuir 24:8695–8700
16. Jeyachandran YL, Mielczarski JA, Mielczarski E, Rai B (2010) Efficiency of blocking of non-specific interaction of different proteins by BSA adsorbed on hydrophobic and hydrophilic surfaces. J Colloid Interface Sci 341:136–142
17. Berman HM, Westbrook J, Feng Z, Gilliland G, Bhat TN, Weissig H, Shindyalov IN, Bourne PE (2000) The Protein Data Bank. Nucleic Acids Res 28:235–242
18. Zhang L, Sun Y (2010) Molecular simulation of adsorption and its implications to protein chromatography: a review. Biochem Eng J 48:408–415
19. Brooks BR, Brooks CL, Mackerell AD, Nilsson L, Petrella RJ, Roux B, Won Y, Archontis G, Bartels C, Boresch S, Caflisch A, Caves L, Cui Q, Dinner AR, Feig M, Fischer S, Gao J, Hodoscek M, Im W, Kuczera K, Lazaridis T, Ma J, Ovchinnikov V, Paci E, Pastor RW, Post CB, Pu JZ, Schaefer M, Tidor B, Venable RM, Woodcock HL, Wu X, Yang W, York DM, Karplus M (2009) CHARMM: the biomolecular simulation program. J Comput Chem 30:1545–1614
20. Jeyachandran YL, Mielezarski E, Rai B, Mielczarski JA (2009) Quantitative and qualitative evaluation of adsorption/desorption of bovine serum albumin on hydrophilic and hydrophobic surfaces. Langmuir 25:11614–11620
21. Villoutreix BO, Renault N, Lagorce D, Sperandio O, Montes M, Miteva MA (2007) Free resources to assist structure-based virtual ligand screening experiments. Curr Protein Pept Sci 8:381–441
22. Cohavi O, Corni S, De Rienzo F, Di Felice R, Gottschalk KE, Hoefling M, Kokh D, Molinari E, Schreiber G, Vaskevich A, Wade RC (2010) Protein–surface interactions: challenging experiments and computations. J Mol Recognit 23:259–262
23. Chen R, Li L, Weng ZP (2003) ZDOCK: an initial-stage protein-docking algorithm. Proteins 52:80–87
24. Wiehe K, Pierce B, Tong WW, Hwang H, Mintseris J, Weng Z (2007) The performance of ZDOCK and ZRANK in rounds 6-11 of CAPRI. Proteins 69:719–725
25. Huang BX, Kim HY, Dass C (2004) Probing three-dimensional structure of bovine serum albumin by chemical cross-linking and mass spectrometry. J Am Soc Mass Spectrosc 15:1237–1247
26. Mashiach E, Nussinov R, Wolfson HJ (2010) Fiber Dock: flexible induced-fit backbone refinement in molecular docking. Proteins 78:1503–1519
27. Chen R, Weng ZP (2002) Docking unbound proteins using shape complementarity, desolvation, and electrostatics. Proteins 47:281–294
28. Lei HT, Shen YD, Song LJ, Yang JY, Chevallier OP, Haughey SA, Wang H, Sun YM, Elliott CT (2010) Hapten synthesis and antibody production for the development of a melamine immunoassay. Anal Chim Acta 665:84–90
29. Yeh LC, Lee WM, Koh BW, Chan JP, Liu CH, Kao JP, Chou CC (2008) Development of amoxicillin enzyme-linked immunosorbent assay and measurements of tissue amoxicillin concentrations in a pigeon microdialysis model. Poult Sci 87:577–587
30. Burmester J, Spinelli S, Pugliese L, Krebber A, Honegger A, Jung S, Schimmele B, Cambillau C, Pluckthun A (2001) Selection, characterization and X-ray structure of anti-ampicillin single-chain Fv fragments from phage-displayed murine antibody libraries. J Mol Biol 309:671–685
31. Comeau SR, Gatchell DW, Vajda S, Camacho CJ (2004) ClusPro: an automated docking and discrimination method for the prediction of protein complexes. Bioinformatics 20:45–50
32. Lorenzen S, Zhang Y (2007) Identification of near-native structures by clustering protein docking conformations. Proteins 68:187–194
33. Sinha N, Mohan S, Lipschultz CA, Smith-Gill SJ (2002) Differences in electrostatic properties at antibody-antigen binding sites: implications for specificity and cross-reactivity. Biophys J 83:2946–2968
34. Pierce B, Weng Z (2007) ZRANK: reranking protein docking predictions with an optimized energy function. Proteins 67:1078–1086
35. Bacigalupo MA, Meroni G, Secundo F, Lelli R (2008) Time-resolved fluoroimmunoassay for quantitative determination of ampicillin in cow milk samples with different fat contents. Talanta 77:126–130
36. Samsonova ZHV, Shchelokova OS, Ivanova NL, Rubtsova MIU, Egorov AM (2005) Enzyme immunoassay of ampicillin in milk. Prikl Biokhim Mikrobiol 41:668–675
37. Zhi ZL, Meyer UJ, van den Bedem JW, Meuse M (2001) Evaluation of an automated and integrated flow-through immunoanalysis system for the rapid determination of cephalexin in raw milk. Anal Chim Acta 442:207–219
38. Chen LB, Wang ZF, Ferreri M, Su JL, Han B (2009) Cephalexin residue detection in milk and beef by ELISA and colloidal gold based one-step strip assay. J Agric Food Chem 57:4674–4679
39. Wu H, Yang WC, Ma J (2008) Determination of penicillin in milk by the electrochemical immunosensor. Chem Bull (Chinese) 71:394–397
40. Thavarungkul P, Dawan S, Kanatharana P, Asawatreratanakul P (2007) Detecting penicillin G in milk with impedimetric label-free immunosensor. Biosens Bioelectron 23:688–694